Article

Single-Molecule Motions of Oligoarginine Transporter Conjugates on the Plasma Membrane of Chinese Hamster Ovary Cells

H.-L. Lee, E. A. Dubikovskaya, H. Hwang, A. N. Semyonov, H. Wang, L. R. Jones, R. J. Twieg, W. E. Moerner, and P. A. Wender

J. Am. Chem. Soc., **2008**, 130 (29), 9364-9370 • DOI: 10.1021/ja710798b • Publication Date (Web): 26 June 2008

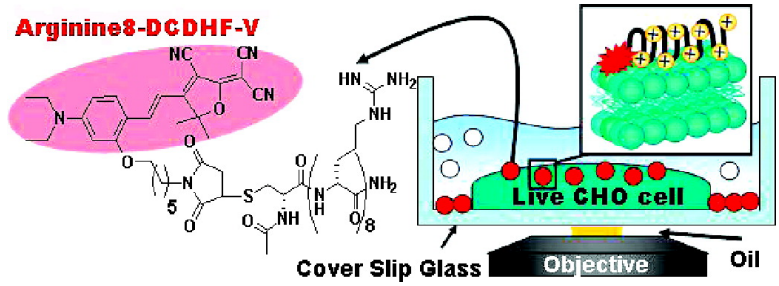

More About This Article

Additional resources and features associated with this article are available within the HTML version:

- Supporting Information
- Access to high resolution figures
- Links to articles and content related to this article
- Copyright permission to reproduce figures and/or text from this article

View the Full Text HTML

J|A|C|S
ARTICLES

Published on Web 06/26/2008

Single-Molecule Motions of Oligoarginine Transporter Conjugates on the Plasma Membrane of Chinese Hamster Ovary Cells

H.-L. Lee,[†] E. A. Dubikovskaya,[†] H. Hwang,[†] A. N. Semyonov,[§] H. Wang,[§] L. R. Jones,[†] R. J. Twieg,[§] W. E. Moerner,*[,†] and P. A. Wender*[,†,‡]

Department of Chemistry and Department of Chemical and Systems Biology, Stanford University, Stanford, California 94305, and Department of Chemistry, Kent State University, Kent, Ohio 44242

Received December 4, 2007; E-mail: wenderp@stanford.edu; wmoerner@stanford.edu

Ⓦ **This paper contains enhanced objects available on the Internet at http://pubs.acs.org/jacs.**

Abstract: To explore the real-time dynamic behavior of molecular transporters of the cell-penetrating-peptide (CPP) type on a biological membrane, single fluorescently labeled oligoarginine conjugates were imaged interacting with the plasma membrane of Chinese hamster ovary (CHO) cells. The diffusional motion on the membrane, characterized by single-molecule diffusion coefficient and residence time (τ_R), defined as the time from the initial appearance of a single-molecule spot on the membrane (from the solution) to the time the single molecule disappears from the imaging focal plane, was observed for a fluorophore-labeled octaarginine (a model guanidinium-rich CPP) and compared with the corresponding values observed for a tetraarginine conjugate (negative control), a lipid analogue, and a fluorescently labeled protein conjugate (transferrin-Alexa594) known to enter the cell through endocytosis. Imaging of the oligoarginine conjugates was enabled by the use of a new high-contrast fluorophore in the dicyanomethylenedihydrofuran family, which brightens upon interaction with the membrane at normal oxygen concentrations. Taken as a whole, the motions of the octaarginine conjugate single molecules are highly heterogeneous and cannot be described as Brownian motion with a single diffusion coefficient. The observed behavior is also different from that of lipids, known to penetrate cellular membranes through passive diffusion, conventionally involving lateral diffusion followed by membrane bilayer flip-flop. Furthermore, while the octaarginine conjugate behavior shares some common features with transferrin uptake (endocytotic) processes, the two systems also exhibit dissimilar traits when diffusional motions and residence times of single constructs are compared. Additionally, pretreatment of cells with cytochalasin D, a known actin filament disruptor, produces no significant effect, which further rules out unimodal endocytosis as the mechanism of uptake. Also, the involvement of membrane potential in octaarginine−membrane interaction is supported by significant changes in the motion with high [K^+] treatment. In sum, this first study of single transporter motion on the membrane of a living cell indicates that the mode by which the octaarginine transporter penetrates the cell membrane appears to either be a multimechanism uptake process or a mechanism different from unimodal passive diffusion or endocytosis.

Introduction

Biological membranes have evolved in part to prevent xenobiotics from passively entering cells.[1] Notwithstanding this barrier function, numerous organisms have developed proteins, many of which are transcription factors, that breach membranes through a variety of mechanisms.[2] The protein HIV tat, for example, when used *in vitro*, rapidly enters the cytosol (and nucleus) of a wide variety of cells by endocytosis.[3] However, the nine-amino-acid peptide required for the uptake of HIV tat, residues 49−57 (RKKRRQRRR), appears to utilize an additional mechanism, as is evident from its uptake, even at 4 °C, by a route distinct from the intact protein,[4] sensitive to the attached cargo size and composition and even to cell type. Our previous studies demonstrated that the guanidinium head groups of tat 49−57 are the key functionalities required for its entry into cells. Indeed, replacement of all non-arginine residues in tat 49−57 with arginines provides molecular transporters that exhibit superior rates of uptake. Charge itself is necessary, but not sufficient, as is evident from the comparatively poor uptake of lysine nonamers.[5,6] Bidentate hydrogen bonding of the

[†] Department of Chemistry, Stanford University.
[§] Department of Chemistry, Kent State University.
[‡] Department of Chemical and Systems Biology, Stanford University.

(1) Alberts, B.; Lewis, J.; Raff, M.; Roberts, K.; Watson, J. *Molecular Biology of the Cell*; Garland: New York, NY, 1994.
(2) Joliot, A.; Prochiantz, A. *Nat. Cell Biol.* **2004**, *6*, 189.
(3) Mann, D. A.; Frankel, A. D. *EMBO J.* **1991**, *10*, 1733.
(4) Silhol, M.; Tyagi, M.; Giacca, M.; Lebleu, B.; Vives, E. *Eur. J. Biochem.* **2002**, *269*, 494.
(5) Wender P. A. MitchellD. J. PattabiramanK. PelkeyE. T. Steinman L. RothbardJ. B. *Proc. Natl. Acad. Sci. U.S.A.* **2000**, *97*, 13003. Wender, P. A.; Galliher, W. C.; Goun, E. A.; Jones, L. R.; Pillow, T. H. *Adv. Drug Deliv. Rev.* **2008**, *60*, 452.
(6) Goun, E. A.; Pillow, T. H.; Jones, L. R.; Rothbard, J. B.; Wender, P. A. *ChemBioChem* **2006**, *7*, 1497.

10.1021/ja710798b CCC: $40.75

cationic guanidinium groups to anionic cell surface groups (phosphates, carboxylates, sulfates) is important, as indicated by the finding that mono- or dimethylation of the critical guanidinium groups, while preserving charge, reduces or eliminates uptake. The number of arginines and therefore guanidinium groups is also important, with optimal uptake for oligomers of 7−15 residues.[6,7] Natural backbone chirality is not critical for uptake, as the unnatural peptides show increased uptake relative to the natural peptides. Even the position of attachment and length of the side chains can be altered, as shown, for example, with guanidinium-rich peptoids that exhibit highly efficient uptake.[5] Changes in the backbone composition and in the side-chain spacing between residues also can increase uptake, with highly branched, guanidinium-rich oligosaccharides and dendrimers being efficient transporters.[5,6,8–10] In contrast to receptor-mediated uptake, an increase in conformational flexibility of the guanidinium-rich transporters generally enhances uptake.

Several mechanisms could accommodate the above structure−function relationships for guanidinium-rich cell-penetrating peptides (CPPs) and, more generally, guanidinium-rich molecular transporters (GRTs).[5,6,11] These mechanisms could even operate concurrently, depending on, for example, the properties of the CPPs and cargoes, CCP concentrations, the choice of selected cell lines, and assay conditions. A receptor-mediated process is inconsistent with the broad range of structural modifications that promote uptake and especially the observation that more-flexible systems show enhanced uptake. Endocytosis and macropinocytosis have been proposed and appear to be pertinent to entry involving high-molecular-weight CPP conjugates.[11,18,19] Conventional passive diffusion across the nonpolar interior of the plasma membrane is seemingly difficult to reconcile with the polarity of the arginine oligomers (which are highly water soluble) and the dependency of uptake on the number of charges. However, our prior studies have suggested that an adaptive translocation mechanism might be operative for low-molecular-weight guanidinium-based conjugates.[6,11,12] In this process, positively charged guanidinium oligomers, which alone are too polar to enter a membrane, form bidentate hydrogen-bonded ion-pair complexes with complementary charged cell surface functionalities of membrane-embedded groups (carboxylates, sulfates, phosphates) and are driven inward across the membrane under the influence of the membrane potential. It is especially noteworthy, with respect to this mechanism, that water-soluble arginine oligomers can be completely solubilized in octanol (a membrane dielectric mimic) by treatment with an equivalent of a fatty acid salt (sodium laurate).[12]

Various CPPs have been reported to carry exogenous molecules into cells.[6,7,10,11] Understanding the internalization mechanism of peptide transporters is fundamental to their use as delivery vectors for drugs and probes, especially in view of the increasing interest in the delivery of biologicals (peptides, proteins, nucleic acids, etc). To address the recent controversy surrounding the uptake mechanism of arginine-rich CPP peptides,[13–19] we decided to examine, by direct observation in real time, their membrane interactions on a single-molecule level in living cells.

Single-molecule imaging is a technique that has been used to probe the dynamics of molecules as well as their local environments in liquids, solids, surfaces, and living cell membranes.[20–25] Unlike assays used in previous studies, this technique can be used to directly observe the motion of individual oligoarginines in real time rather than the motion inferred indirectly from the behavior of the ensemble average. Attempting to indirectly define the behavior on the basis of the average alone makes analysis extremely complex and open to a number of different interpretations, particularly when multiple mechanisms might be operating concurrently.[15,17,18] This work is the first report describing the direct observation of the motion of CPPs on the plasma membrane in real time on a single-molecule level in living cells.

In this investigation, epifluorescence imaging is used to study the movement of single fluorophore-labeled octaarginine transporters using living Chinese hamster ovary (CHO) cells.[26–29] A novel label, the DCDHF-V fluorophore, is used which belongs to a class of single-molecule fluorophores consisting of an amine donor and dicyanomethylenedihydrofuran (DCDHF) acceptor linked by a conjugated unit (e.g., benzene, naphthalene, styrene, etc.). Molecules in the DCDHF class exhibit useful properties for single-molecule studies, such as high quantum yields, photostability, and environmental reporter functions.[26–29] DCDHF-V, with conjugation extended by an additional vinyl group, absorbs and emits at long wavelengths ($\lambda_{ex} = 610$ nm, $\lambda_{em} = 630$ nm in water), thereby avoiding cellular autofluorescence. Here, a maleimide derivative of DCDHF-V is covalently attached to the octaarginine backbone through an N-terminal cysteine; as such, it reports on the mobility of the resultant

(7) Futaki, S.; Suzuki, T.; Ohashi, W.; Yagami, T.; Tanaka, S.; Ueda, K.; Sugiura, Y. *J. Biol. Chem.* **2001**, *276*, 5836.
(8) Elson-Schwab, L.; Garner, O. B.; Schuksz, M.; Esko, J. D.; Tor, Y. *J. Biol. Chem.* **2007**, *282*, 13585.
(9) Futaki, S.; Nakase, I.; Suzuki, T.; Youjun, Z.; Sugiura, Y. *Biochemistry* **2002**, *41*, 7925.
(10) Chung, H. H.; Harms, G.; Seong, C. M.; Choi, B. H.; Min, C.; Taulane, J. P.; Goodman, M. *Biopolymers* **2004**, *76*, 83.
(11) Rothbard, J. B.; Jessop, T. C.; Wender, P. A. *Adv. Drug Deliv. Rev.* **2005**, *57*, 495.
(12) Rothbard, J. B.; Jessop, T. C.; Lewis, R. S.; Murray, B. A.; Wender, P. A. *J. Am. Chem. Soc.* **2004**, *126*, 9506.
(13) Fretz, M.; Jin, J.; Conibere, R.; Penning, N. A.; Al-Taei, S.; Storm, G.; Futaki, S.; Takeuchi, T.; Nakase, I.; Jones, A. T. *J. Controlled Release* **2006**, *116*, 247.
(14) Zaro, J. L.; Rajapaksa, T. E.; Okamoto, C. T.; Shen, W.-C. *Mol. Pharm.* **2006**, *3*, 181.
(15) Nakase, I.; Niwa, M.; Takeuchi, T.; Sonomura, K.; Kawabata, N.; Koike, Y.; Takehashi, M.; Tanaka, S.; Ueda, K.; Simpson, J. C.; Jones, A. T.; Sugiura, Y.; Futaki, S. *Mol. Ther.* **2004**, *10*, 1011.
(16) Fischer, R.; Kohler, K.; Fotin-Mleczek, M.; Brock, R. A. *J. Biol. Chem.* **2004**, *279*, 12625.
(17) Suzuki, T.; Futaki, S.; Niwa, M.; Tanaka, S.; Sugiura, Y. *J. Biol. Chem.* **2002**, *277*, 2437.
(18) Futaki, S. *Adv. Drug Deliv. Rev.* **2005**, *57*, 547.
(19) Maiolo, J. R.; Ferrer, M.; Ottinger, E. A. *Biochim. Biophys. Acta−Biomembranes* **2005**, *1712*, 161.
(20) Dickson, R. M.; Norris, D. J.; Tzeng, Y.-L.; Moerner, W. E. *Science* **1996**, *274*, 966.
(21) Nie, S.; Zare, R. N. *Annu. Rev. Biophys. Biomol. Struct.* **1997**, *26*, 567.
(22) Moerner, W. E.; Orrit, M. *Science* **1999**, *283*, 1670.
(23) Sako, Y.; Minoguchi, S.; Yanagida, T. *Nat. Cell Biol.* **2000**, *2*, 168.
(24) Nishimura, S. Y.; Vrljic, M.; Klein, L. O.; McConnell, H. M.; Moerner, W. E. *Biophys. J.* **2006**, *90*, 927.
(25) Moerner, W. E. *J. Phys. Chem. B* **2002**, *106*, 910.
(26) Willets, K. A.; Ostroverkhova, O.; He, M.; Twieg, R. J.; Moerner, W. E. *J. Am. Chem. Soc.* **2003**, *125*, 1174.
(27) Willets, K. A.; Nishimura, S. Y.; Schuck, P. J.; Twieg, R. J.; Moerner, W. E. *Acc. Chem. Res.* **2005**, *38*, 549.
(28) Willets, K. A.; Callis, P.; Moerner, W. E. *J. Phys. Chem. B* **2004**, *108*, 10465.
(29) Nishimura, S. Y.; Lord, S. J.; Klein, L. O.; Willets, K. A.; He, M.; Lu, Z.; Twieg, R. J.; Moerner, W. E. *J. Phys. Chem. B* **2006**, *110*, 8151.

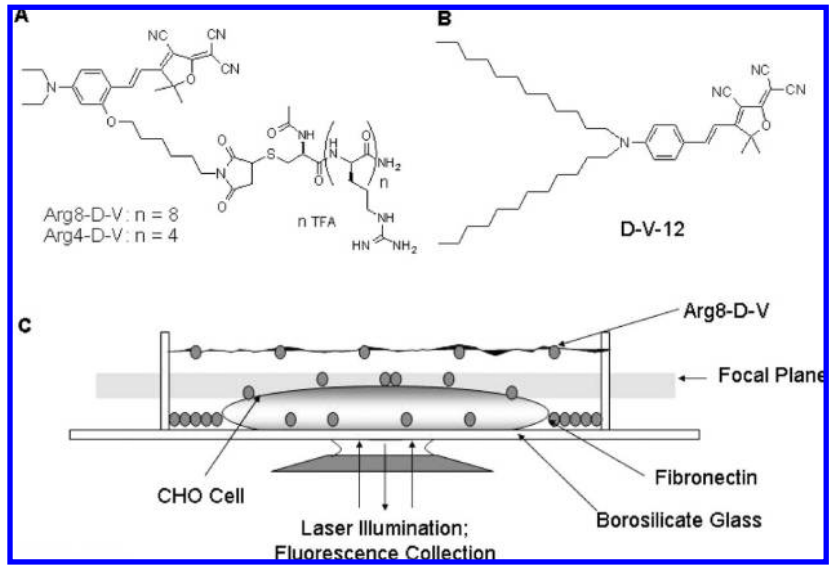

Figure 1. (A) Structures of DCDHF-V labeled octaarginine (Arg8-D-V) and tetraarginine (Arg4-D-V). (B) Structure of DCDHF-V-labeled lipid analogue (D-V-12). (C) Schematic of the imaging arrangement. CHO cells were cultured in fibronectin-coated imaging chambers and examined on an inverted epifluorescence microscope. The focal plane of the microscope is indicated. For details, see Experimental Section and Supporting Information.

octaarginine peptide conjugate (see Figure 1A). This fluorophore is brighter when the molecule is interacting with the more constrained environment of the membrane (and the cell interior) compared to the aqueous buffer outside the cell; hence, contrast in single-molecule imaging is enhanced. Moreover, useful signal-to-background is obtained at physiological oxygen concentrations, and the contrast observed is superior to that of the Cy3 dye (Amersham) with or without oxygen scavengers. Our results indicate that the behavior of octaarginine on a cell surface is different from that of lipids, known to penetrate cellular membranes through passive diffusion, conventionally involving lateral diffusion followed by membrane flip-flop. Furthermore, while the octaarginine behavior shares some common features with protein uptake (endocytotic) processes, it also exhibits dissimilar diffusion properties at the single-molecule level. The mode by which octaarginine penetrates the cell membrane appears to be either a multimechanism uptake process or a mechanism different from passive diffusion and endocytosis. These results have relevance to the mechanism of cellular uptake of guanidinium-rich transporters conjugated to small molecules, drugs, and probes (MW ca. <3000).

Experimental Section

Synthesis of the Conjugates. The preparation of the DCDHF-V maleimide, its peptide conjugates, and the lipid analogue D-V-12 are detailed in the Supporting Information. The synthesis of DCDHF-V has been previously reported.[33–35] The transferrin-Alexa594 conjugate was purchased from Molecular Probes (Eugene, OR).

CHO Cell Culture and Imaging Conditions. 1. Common Procedures. For details of cell culture, see ref 31. Briefly, cells were imaged at 22 °C in phosphate-buffered saline (PBS, pH 7.2), while treatments with different drugs, prior to imaging, were done at 37 °C. Unless mentioned otherwise, 1 nM of Arg8-D-V conjugates in PBS buffer was applied to the CHO cells for observing single molecules. Imaging was performed within 1 h after removing the cell tray from the 37 °C incubator to ensure the viability of the cells. During imaging, the conjugates and/or the drugs remained in solution.

2. Arg8-D-V on PEM. Polyelectrolyte multilayers (PEM) were used to immobilize Arg8-D-V in an aqueous (pH 8) environment in order to mimic the binding of Arg8-D-V on the CHO plasma membrane. Sequential deposition of poly(acrylic acid) (PAcr, Aldrich Chemical, Milwaukee, WI) and polyethyleneimine (PEI, Sigma, St. Louis, MO,) has been shown to reduce nonspecific binding of proteins to glass slides,[36] while the uppermost negatively charged PAcr layer immobilizes the cationic Arg8-D-V without dissociation or movement during imaging.

3. D-V-12. D-V-12, the didodecylamine analogue of diethylamine containing DCDHF-V, was stored in chloroform (1 mg/mL stock). Immediately before use, 1−5 μL of D-V-12 stock solution was dried into a film and then reconstituted in 20−100 μL of ethanol. CHO cells were incubated with a final concentration of 100 nM−1 μM of D-V-12 for 10−20 min at 37 °C in supplemented RPMI 1640 media with fetal calf serum. The maximum concentration of ethanol during incubation was 1% v/v.

4. Transferrin-Alexa594. The behaviors of transferrin-Alexa594 molecules on the CHO plasma membrane under conditions that permitted endocytosis were compared with those of Arg8-D-V molecules. Imaging conditions were the same as for Arg8-D-V on CHO cells, except that the concentration of transferrin-Alexa594 was 0.01 nM for tracking individual molecules.

5. High Potassium Ion Concentrations. High-potassium-concentration buffer incubations (high [K^+], 140 mM in PBS) were used to reduce the membrane potential, a treatment which prevented poly(arginine) cellular entry in bulk experiments.[11]

6. Cytochalasin D. For actin depolymerization, cells were treated by incubation with 10 μM cytochalasin D (Sigma) for 30 min at 37 °C. The effect of cytochalasin D has been described elsewhere.[15,17]

7. Amilioride Treatment. Incubation with serum-free medium containing 100 μM amilioride for 60 min at 37 °C, followed by washing with PBS buffer, was used to inhibit macropinocytosis.[14,15]

(30) Elowitz, M. B.; Surette, M. G.; Wolf, P-E.; Stock, J. B.; Leibler, S. *J. Bacteriol.* **1999**, *181*, 197.
(31) Vrljic, M.; Nishimura, S. Y.; Brasselet, S.; Moerner, W. E.; McConnell, H. M. *Biophys. J.* **2002**, *83*, 2681.
(32) Qian, H.; Sheetz, M P.; Elson, E. L. *Biophys. J.* **1991**, *60*, 910.
(33) Wang, H.; Lu, Z.; Lord, S. J.; Willets, K. A.; Bunge, S.; Moerner, W. E.; Twieg, R. J. *Tetrahedron* **2007**, *63*, 103.

8. Excess Arg8 Peptide Treatment. Excess unlabeled octaarginines (Arg8 peptide, at 10 μM) were mixed with Arg8-D-V (1 nM) and together applied to the CHO cells for imaging.

Single-Molecule Fluorescence Imaging of Trajectories. The fluorescence from individual molecules was recorded using the standard methods of single-molecule, wide-field epifluorescence imaging (see Supporting Information). Except in the case of D-V-12 (20 ms) and transferrin-Alexa594 (100 ms), all movies were recorded at 50 ms integration time with continuous illumination. Laser light at 532 nm was used for imaging of D-V-12, while 594 nm laser light was used for imaging of Arg8-D-V, Arg4-D-V, and transferrin-Alexa594.

CHO cells adhere well to the glass surface of the chambered coverglass, becoming spindly with dimensions of $\sim 30 \times 10 \times 5$ μm. Thus, the bottom and the top portions of the plasma membrane are parallel to the focal plane of the microscope and can be treated as two-dimensional planes (see Figure 1). Near the edges of the cell, out-of-focal-plane diffusion can occur and could be detected by an increase in the spot size. It is well-known that the bottom membrane of the cell contains adhesions that could restrict or perturb the trajectories of single molecules. Therefore, only single molecules located on the upper surface of the cell and away from cell edges were included in the analyses.

The successive (x,y) positions of the single molecules on the plane of the cell surface were recorded as a function of time. In order to investigate the behavior of single conjugates in a consistent fashion, only the fluorescent spots that appeared after the start of illumination and disappeared before the end of recording were considered. The residence time (τ_R) is defined as the time of visibility from the initial appearance of a single-molecule spot on the membrane (from the solution) to the time the single molecule disappears from the imaging focal plane in a single frame. The diffusion coefficients for each trajectory were extracted as described in the Supporting Information.

Results

The experimental data consist primarily of high-speed microscopic imaging of the motion of single fluorescently labeled molecules on the plasma membrane of CHO cells. A schematic of the epifluorescence imaging arrangement is shown in Figure 1C, emphasizing that the focal plane of the microscope was most often located at the upper plasma membrane. For details, see Experimental Section and Supporting Information.

Fluorescently Labeled Arg8 Conjugates Are Readily Internalized, and Single Copies Can Be Observed Interacting with the Plasma Membrane. Figure 2A shows a wide-field epifluorescence image of two CHO cells which have been incubated with a high concentration of Arg8-D-V (5 μM). The focal plane was placed near the center (equatorial plane) of the cell for this image only. The bright fluorescent regions confirm that many internalized, labeled peptides are easily seen in the cell interior, in various stages of interaction with organelles. The constructs are also concentrated at the plasma membrane and do not enter the nucleus. The ease of uptake of the Arg8 construct is consistent with earlier reports.[4–19]

Figure 2B shows the upper plasma membrane, where the cell has been incubated with a lower concentration of Arg8-D-V (10 nM). Now the fluorophore-labeled peptides appear as fluorescent spots. In Figure 2C, at 1 nM incubation, isolated, individual molecules are clearly observed (see video). These are seen to disappear in a single frame and have brightness representative of single copies of the DCDHF-V emitter (data not shown). It is worth noting that the high contrast of this image is a result of the use of the DCDHF-V label, which has quenched fluorescence in the lower viscosity environment of the buffer solution above the cell, yet becomes bright in constrained and

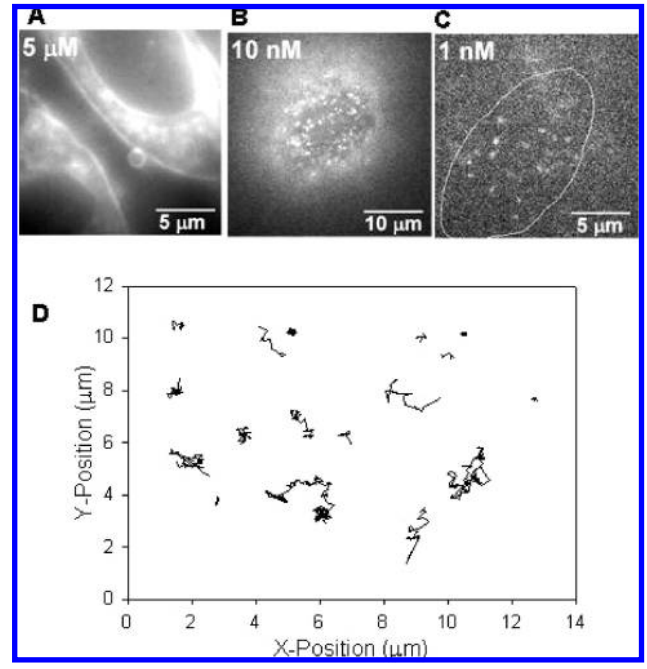

Figure 2. (A−C) Representative images of Arg8-D-V on the CHO plasma membrane with decreasing concentration of conjugate. (D) Representative trajectories of single Arg8-D-V conjugates on the CHO plasma membrane.

Ⓦ A video in AVI format, showing the motion of the molecules in panel C, is available.

hydrophobic environments,[29] for example, when the Arg8-D-V constructs are interacting with the plasma membrane.

The behavior of the DCDHF-V label also becomes apparent when the oxygen concentration is lowered by an enzymatic oxygen scavenger system with β-mercaptoethanol, often used to extend the photobleaching time of fluorophores (see Experimental Section). In separate studies of this treatment in gels (see Supporting Information), the photobleaching time of DCDHF-V increases, but severe blinking also occurs on the 100 ms time scale. More importantly for the present study, at reduced oxygen concentration, the fast-diffusing labeled peptides in solution above the cell now become visible as a background haze (data in Supporting Information). This is likely due to an alteration in photophysical parameters (such as the triplet lifetime), which will be examined in future work. The net effect is that, with lowered oxygen concentration, the contrast of the single-molecule spots in the membrane is greatly reduced due to out-of-focus fluorescence. Similar low-contrast images were also observed when the Arg8 peptide was labeled with Cy3, with or without oxygen scavenger. While background fluorescence could be reduced by confocal imaging or other methods, by using the DCDHF-V label, the simplicity, parallelism, and speed of wide-field epifluorescence imaging is maintained under conditions of normal oxygen concentration, with higher contrast than is available with Cy3.

By acquiring images like Figure 2C at the frame exposure time of 20−100 ms per image and extracting the positions of the single-molecule spots as a function of time, single-molecule position trajectories are obtained. Figure 2D shows some representative examples, placed at different positions in the plane for clarity. This motion is not due to molecules in solution above the cell, because it is much slower than that of free conjugates. It is also well-known that cytoplasmic diffusion is, in general, faster than in-membrane diffusion. For example, a cytoplasmic diffusion coefficient for GFP of ~ 8 $\mu m^2/s$ has been

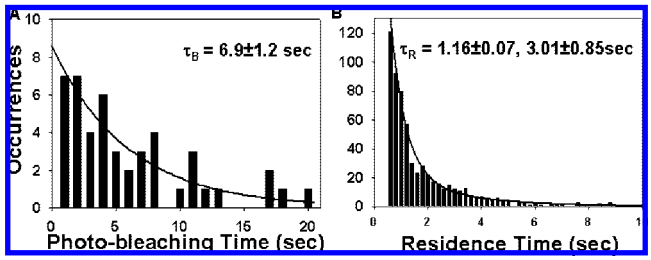

Figure 3. Comparison of photobleaching time τ_B and residence time τ_R. (A) Histogram of photobleaching times for single Arg8-D-V on PEM. (B) Histogram of residence times for Arg8-D-V on CHO cells. The pump wavelength is 594 nm, with a pumping intensity of 140 W/cm^2.

reported,[30] much faster than the diffusion coefficients we observe (*vide infra*). For these reasons, it is reasonable to regard the trajectories in Figure 2D as on-membrane motion. However, since the focal depth of the microscope is ~300 nm, we cannot completely exclude the possibility that some of the observed motion represents motion in the cytoplasm below the membrane.

A key goal of this work is to characterize these motions in a quantitative fashion by analysis of the individual trajectories and to compare these characteristics across the panel of various transporters (octaarginine, tetraarginine, lipid, and the protein transferrin). Examination of Figure 2D suggests that the motions observed for single molecules of the octaarginine transporter are quite heterogeneous. Some molecules move very little, others appear to undergo random motion over larger distances, and some make large initial displacements before more random explorations (e.g., the molecule at $x = 9$ μm and $y = 2.5$ μm). While this last behavior is quite intriguing, it was relatively rare and thus was not further analyzed.

Single Arg8-D-V Molecules Typically Disappear from the Images before Photobleaching. The first quantity of interest is the residence time, τ_R, in or near the plasma membrane, defined above. A molecule might disappear for several reasons: destruction of the DCDHF-V label due to photobleaching, motion out of the depth of focus of the microscope of ~300 nm, which can occur due to dissociation away from the cell surface, or internalization into the cell.

To quantify the photobleaching behavior, single molecules of Arg8-D-V were imaged on a poly(electrolyte) multilayer (PEM) in (normally oxygenated) buffer as an approximate model for the confined and charged membrane environment. Under these conditions, the time to photobleaching, τ_B, was recorded, yielding the τ_B distribution in Figure 3A. For the same molecules, the total number of detected photons from each emitter was determined by integration of a small area containing all the photons from the molecule, with background subtracted; the average is $(8.3 \pm 1.1) \times 10^4$. A single exponential fit to the τ_B data (expected for Poisson statistics) was observed, yielding an average τ_B of 6.9 ± 1.2 s. While the DCDHF-V molecules may last longer in a completely oxygen-free environment or in a polymeric host,[27] this measurement provides a reasonable assessment of the photostability of Arg8-D-V under our aqueous, oxygenated cellular imaging conditions.

In contrast, Figure 3B shows the observed residence time τ_R for single molecules of Arg8-D-V on the CHO cell membrane. Each single molecule was followed frame-by-frame as it moved in order to record the total number of detected photons and to determine the total time before disappearance. A double-exponential fit to the τ_R distribution yields characteristic times of 1.16 ± 0.07 and 3 ± 1 s; under these conditions, the average number of detected photons per emitter is $(4.4 \pm 0.61) \times 10^4$. The long-time tail of the τ_R distribution may arise from photobleaching, but the faster component cannot be, and it is reasonable to interpret the disappearance of single molecules in the fast population as dissociation or internalization rather than photobleaching. The fraction actually internalized was not determined in this work, but Figure 2A shows that internalization readily occurs, which is consistent with earlier reports.[4–19] Residence time distributions were also obtained for D-V-12, transferrin-Alexa594, Arg4-D-V, and Arg8-D-V on CHO cells treated with high [K$^+$] buffer, and single-exponential behavior was observed for all cases except the last (see Supporting Information and Table 1).

Table 1. Tabulated Values for Residence Time, Average Diffusion Coefficients, and Number of Particles Tracked (*N*) for Transferrin-Alexa594 Conjugate, Arg8-D-V, Arg8-D-V in High [K$^+$], Arg4-D-V, and D-V-12 on the CHO Plasma Membrane

experiment	τ_R, s (*N*)	D_{avg}, μm^2/s (*N*)
transferrin-Alexa594	4.04 ± 0.22 (211)[a]	0.062 ± 0.005 (202)
Arg8-D-V, cytochalasin D	1.58 ± 0.24 (298)[b]	0.16 ± 0.01 (287)
Arg8-D-V	1.16 ± 0.07 (627)[b]	0.17 ± 0.01 (570)
Arg8-D-V, high [K$^+$]	1.15 ± 0.09 (481)[b]	0.22 ± 0.01 (447)
Arg4-D-V	0.79 ± 0.03 (50)	*c*
D-V-12	0.54 ± 0.01 (152)	1.87 ± 0.12 (134)

[a] Lower limit; may be limited by photobleaching. [b] Shorter of two time constants. [c] Insufficient data.

Diffusion Coefficients of Single-Molecule Trajectories. The positional trajectories of single molecules allow analysis of the motion to determine if the constructs move randomly on the surface by unconstrained Brownian motion, or move in some other way. To do this in an unbiased fashion, each trajectory was truncated to 10 time steps so that all molecules would have the same trajectory length, and *D* values were extracted from mean-squared displacements as described in the Supporting Information and displayed in Figure 4. Since the trajectories are finite in length, naturally there is a statistical error in each *D* determination. To be as unbiased as possible, we compare the measured *D* distributions with the simplest hypothesis, i.e., that all measured values arise from underlying random Brownian motion with a single diffusion coefficient, D_o. Under this homogeneity hypothesis, the measured single-molecule *D* values should scatter according to a well-known probability distribution,[31,32] the smooth black curve in each panel. Departures from the distribution indicate heterogeneous motion. Whether or not this hypothesis was upheld, we also computed an ensemble average diffusion coefficient, D_{avg}, from the measurements.

The Motion of Arg8-D-V on CHO Cells Differs Significantly from a Lipid Analogue, an Endocytotic Protein Conjugate, and Arg4-D-V. The membrane-associated motion of the Arg8-D-V construct was examined by extracting distributions of single-molecule diffusion coefficients and residence times, and these values were compared to those obtained from the following cases: (a) a lipid-like derivative of the same fluorophore (D-

(34) Lu, Z.; Weber, R.; Twieg, R. J. *Tetrahedron Lett.* **2006**, *47*, 7213.
(35) He, M.; Twieg, R. J.; Ostroverkhova, O.; Gubler, U.; Wright, D.; Moerner, W. E. *Proc. SPIE* **2002**, *4802*, 9.
(36) Kartalov, E. P.; Unger, M. A.; Quake, S. R. *BioTechniques* **2003**, *34*, 505.

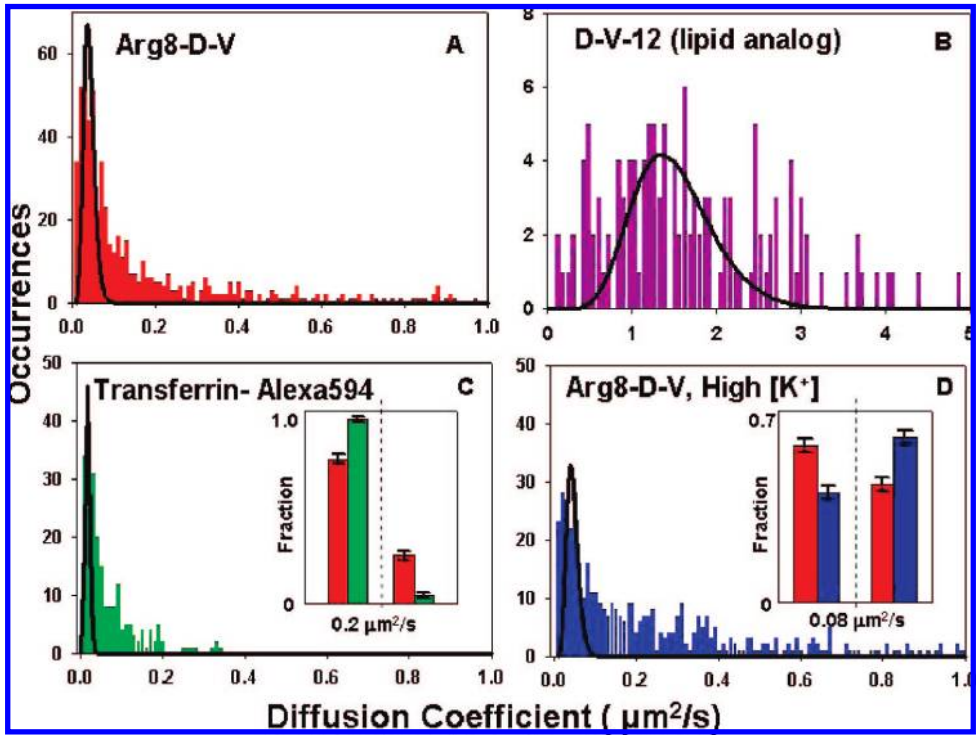

Figure 4. Distributions of single-molecule diffusion coefficients (D) for (A) Arg8-D-V, (B) D-V-12, (C) transferrin-Alexa594 conjugate, and (D) Arg8-D-V in high [K^+] on the CHO plasma membrane. The inset of panel C shows the fraction of molecules below and above a cutoff of 0.2 $\mu m^2/s$ for Arg8-D-V (red) and transferrin-Alexa594 (green). The inset of panel D shows the fraction of molecules below and above a cutoff of 0.08 $\mu m^2/s$ for Arg8-D-V (red) and Arg8-D-V in high [K^+] (blue).

V-12), expected to enter cells via lateral passive diffusion followed by membrane flip-flop mechanism; (b) a labeled protein (transferrin-Alexa594 conjugate) known to penetrate cells via clathrin-mediated endocytosis;[11] and (c) Arg4-D-V, a water-soluble tetraarginine conjugate that, in contrast to octaarginine, is incapable of penetrating or only poorly penetrates the intact plasma membrane.[6,11,12] Treatments of cells prior to imaging were also performed with high [K^+] PBS buffer (140 mM) that is known to reduce membrane potential to close to zero and consequently to reduce uptake of octaarginine conjugates.[6,11] Treatment with amilioride, known to shut down macropinocytosis,[14,15] and addition of excess unlabeled Arg8 were also performed.

Figure 4 compares observed diffusion coefficient distributions for the four primary cases. The difference between the histograms and the solid curves indicates that the motion of the molecules at our imaging rate is inconsistent with homogeneous Brownian diffusion. For the transferrin conjugate (Figure 4C), the motion is heterogeneous, indicating that a variety of diffusional behaviors are present, perhaps due to endocytotic vesicles in various stages of formation. Heterogeneous motion occurs even more dramatically for the Arg8-D-V conjugate (Figure 4A), where a long tail to high D values is present. This may reflect the binding of the positively charged guanidinium groups to varying numbers of lipids or proteoglycans with negatively charged head groups. The average diffusion coefficient for Arg8-D-V (0.15 ± 0.20 $\mu m^2/s$) is similar to that of MHCII transmembrane proteins in the CHO cell membrane at 22 °C of ~0.2 $\mu m^2/s$.[31]

In contrast, the motion of the lipid analogue (Figure 4B) is closer to homogeneous Brownian diffusion, as was observed earlier for other lipid-like DCDHF derivatives.[29] The average diffusion coefficient of 1.9 $\mu m^2/s$ is similar to that observed for other lipids in the CHO cell membrane at 22 °C.[29] Because the lipids move quickly, the residence times are quite small, mostly due to motion of the molecules out of the observation region.

Comparing diffusion coefficients and τ_R values in Table 1, both the single transferrin proteins and the Arg8-D-V molecules move much more slowly than D-V-12. Transferrin shows even slower diffusion on the membrane, with large residence times, and is known to internalize by formation of a receptor-mediated endocytotic vesicle.[19] Moreover, the motion of Arg8-D-V is different from that of transferrin in two ways. First, the residence time distribution shows shorter values for Arg8-D-V, and second, the Arg8-D-V molecules have a longer tail to larger diffusion coefficients. To show this more directly, we chose an arbitrary D value of 0.2 $\mu m^2/s$, and the fraction of molecules below and above this value are shown in Figure 4C inset. The CPP conjugate has a much larger fraction of molecules with high D values.

In previous studies, tetraarginine (Arg4) was shown to be much less efficient in facilitating cell entry compared to octaarginine.[6,11,12] In comparison to Arg8-D-V, the Arg4-D-V residence times are much shorter (see Supporting Information). This is consistent with a more rapid dissociation of Arg4-D-V from the cell surface due to the lower number of possible ionic interactions.

High [K^+] in the extracellular region is used to reduce the membrane potential and uptake of polyarginine.[6,11] The D distribution for Arg8-D-V with this treatment is changed somewhat compared to that for the normal cell (Figure 4A,D). To explore the changes more carefully, we have constructed normalized probability distributions from the two data sets, which show a relative reduction of the species with lower diffusion coefficients and an increase in the species with higher

diffusion coefficients with high [K^+] treatment (see Supporting Information). To illustrate this approximately, if an arbitrary cutoff is selected, for example, at 0.080 $\mu m^2/s$, the fraction of molecules above and below this value is shown in Figure 4D inset for the normal cell and for high [K^+]. It appears that the reduction in membrane potential causes Arg8-D-V to move faster laterally on the membrane surface and skews the distribution of Arg8-D-V away from that for the endocytotic transferrin construct. However, the residence times of Arg8-D-V on the CHO cell plasma membrane are not changed dramatically with high [K^+] (see Supporting Information).

Treatment with a commonly used suppressor of macropinocytosis, amilioride, was also performed. However, multiple attempts to observe single molecules on the CHO plasma membrane after amilioride treatment were not successful. This is not too surprising, because amilioride treatment affects not only macropinocytosis but also various ion channels, cell morphology, and membrane potential.[13]

Furthermore, treatment of cells with cytochalasin D, a known actin filament disruptor, was performed to investigate the possible involvement of endocytosis.[15,17] Under this treatment, the D_{avg} and D distributions of Arg8-D-V do not change significantly (Table 1). Also, the residence times are relatively close to one another. To further explore the possible effects of cytochalasin D, normalized distributions from the two data sets were also constructed and compared (Figure S4, Supporting Information) as in the case of high [K^+] buffer. Using an arbitrary cutoff at 0.050 $\mu m^2/s$, the relative fractions above and below this cutoff remain unchanged by the cytochalasin D treatment, unlike the case for high [K^+] buffer. From the aforementioned results, we infer that actin polymerization, a vital step in endocytosis, does not play a major role in Arg8-D-V interactions with the plasma membrane in the regime of nanomolar concentrations.

Finally, treatment of cells with an excess level of unlabeled Arg8 peptides ($\sim$10 μM), known to stimulate macropinocytosis,[37] was performed. With this treatment, the D distribution for Arg8-D-V skews slightly to lower diffusion coefficients (Figure S5, Supporting Information). Also, the residence time of Arg8-D-V is reduced by a factor of almost 2 by the treatment with excess Arg8 peptide. In light of these findings, we infer that a high concentration of Arg8 ($\sim$10 μM) may magnify one or more specific modes of interaction with the plasma membrane compared to nanomolar concentrations of Arg8. However, it is not possible to distinguish, at this point, between possibly enhanced macropinocytosis or more efficient penetration by complexes of Arg8 peptides. This effect should be examined in future studies.

(37) Khalil, I. A.; Kogure, K.; Futaki, S.; Harashima, H. *J. Biol. Chem.* **2006**, *281*, 3544.

Conclusions

Our results represent the first report where plasma membrane interactions of a CPP are examined on a single-molecule level in living cells. This study was enabled by the use of a new high-contrast DCDHF fluorophore, which brightens upon interactions with the membrane and provides good contrast under oxygenated conditions. The primary quantities extracted were the residence times of single molecules on the membrane and the single-molecule diffusion coefficients, quantities that cannot be extracted from ensemble measurements. Our findings indicate that the motions of the octaarginine conjugate are highly heterogeneous and cannot be described as Brownian motion with a single diffusion coefficient. The observed motions for the octaarginine constructs are different from those of lipids, known to penetrate cellular membranes through passive diffusion. Furthermore, while the octaarginine behavior shares some common features with transferrin uptake (endocytotic) processes, it also exhibits dissimilar traits when diffusional motions of single constructs are compared. Not only were much larger diffusion coefficients observed for Arg8-D-V, but also the residence times were far smaller than those for transferrin. Suppression of the membrane potential slightly skewed the diffusion coefficient distribution to higher D values. Pretreatment of cells with cytochalasin D, a known actin filament disruptor, does not change the D distribution, which rules out unimodal endocytosis as the mechanism of uptake. Additionally, treatment with excess unlabeled Arg8 peptides (10 μM) favors macropinocytosis or aggregation-enhanced uptake processes. In summary, our real-time, single-molecule analysis suggests that the mode by which octaarginine conjugates penetrate the cell membrane appears to be either a multimechanism uptake process or a mechanism different from passive diffusion and endocytosis. These results have relevance to the mechanism of cellular uptake of guanidinium-rich transporters conjugated to small molecules, drugs, and probes (MW ca. $<$3000).

Acknowledgment. We thank Andrea Kurtz for assistance with PEM preparation, and Adam Cohen, Stefanie Nishimura, and So Yeon Kim for helpful assistance. This work was supported in part by the National Institutes of Health through the NIH Roadmap for Medical Research Grant No. HG003638 (W.E.M., R.J.T.) and by Grants Nos. CA31841 and CA31845 (P.A.W.).

Supporting Information Available: Cell culture, single-molecule imaging and analysis, analysis of motion, synthesis and characterization of probes, additional supporting figures, and additional references. This material is available free of charge via the Internet at http://pubs.acs.org.

JA710798B